P H Y S I C A L   R E V I E W   L E T T E R S

Violation of the Franck-Condon Principle due to Recoil Effects in High Energy Molecular Core-Level Photoionization

E. Kukk,[1,2,*] K. Ueda,[1,†] U. Hergenhahn,[1,3] X.-J. Liu,[1] G. Prümper,[1] H. Yoshida,[4] Y. Tamenori,[5] C. Makochekanwa,[6,7] T. Tanaka,[6] M. Kitajima,[6] and H. Tanaka[6]

[1]*Institute of Multidisciplinary Research for Advanced Materials, Tohoku University, Sendai 980-8577, Japan*
[2]*Department of Physics, University of Turku, FIN-20014, Turku, Finland*
[3]*Max-Planck-Institut für Plasmaphysik, EURATOM Association, 85748 Garching, Germany*
[4]*Department of Chemistry, Hiroshima University, Higashi-Hiroshima 739-8526, Japan*
[5]*Japan Synchrotron Radiation Research Institute, Sayo-gun, Hyogo 679-5198, Japan*
[6]*Department of Physics, Sophia University, Tokyo 102-8554, Japan*
[7]*Graduate School of Sciences, Kyushu University, Fukuoka 812-8581, Japan*
(Received 11 March 2005; published 21 September 2005)

Carbon 1s photoelectron spectra of methane are measured over a photon energy range between 480 eV and 1200 eV. Additional components appear between the individual symmetric stretching vibrational components and are attributed to the excitations of asymmetric stretching and bending vibrations due to recoil of the high-energy photoelectron emission. This recoil effect is the evidence for the violation of the Franck-Condon principle which states that neither the positions nor the momenta of the nuclei change during the ionization event.

One of the main historical challenges and goals of gas-phase soft x-ray electron spectroscopy has been accurate determination of the vibrational fine structure in molecular core-level photoemission [1]. Reliable experimental values of vibrational constants and intensity ratios are a prerequisite for determining quantities of fundamental physical and chemical significance, such as ionization energies and chemical shifts [2]. Numerous studies have focused on methane, one of the simplest hydrocarbons [1,3–10]. Both the experimental resolution and the precision of the theoretical calculations have improved dramatically over the last couple of decades, the latest milestone being the advent of the third generation synchrotron light sources [10,11].

Core-level photoelectron spectra are often used to determine the Franck-Condon factors between the ground and core-ionized states. However, there are a number of effects that can distort the result, such as the post-collision interaction (PCI) and the influence of shape resonances or of the Cooper minimum [12]. With the state-of-the-art electron spectroscopic tools, the accuracy of spectroscopic parameters obtained from the experiment is limited not only by the statistical uncertainties, but rather by how completely all additional effects are accounted for. Thus, it is important to understand all physical processes that accompany the primary event of core ionization. In this Letter, the C 1s photoemission from methane is studied over a broad photon energy range. We demonstrate the presence of non-Franck-Condon effects even well above the ionization threshold and offer a theoretical explanation for the observed long-range increase of the intensity ratios, based on photoelectron recoil effects.

The experiment was carried out at the beam line 27SU at SPring-8 in Japan, which utilizes a figure-8 undulator

[13]. The electron spectra were recorded with Scienta SES-2002 analyzer, mounted with lens axis in horizontal direction. For the high photon energies ($\geq$480 eV) concerned here, the C 1s emission perpendicular to the polarization plane became negligible and the horizontal polarization was used.

A carbon 1s photoelectron spectrum of methane measured at a photon energy $h\nu = 1050$ eV is shown in Fig. 1(b) together with a least-squares curve-fitting decomposition [14] into a single vibrational progression of the symmetric stretching mode ν_s. A Lorentzian width of 95 meV [8] was used for the Voigt profiles. The instrumental broadening was determined from Ar 2p photoelectron spectra and was convoluted with the Doppler broadening (80 meV) to obtain the Gaussian widths (160 meV) of the profiles. A constant vibrational spacing of 397 meV was used, and peak intensities were free parameters of the fit. For comparison, the spectrum recorded at $h\nu = 360$ eV, reported in [15], is also shown in Fig. 1(a). Here, a convolution of a Gaussian profile (69 meV in FWHM) with a PCI-distorted line profile was used for the peak fit. It is clear that the high-energy spectrum is modeled less satisfactorily than the lower-energy spectrum, particularly in the regions between the peaks. This suggests that the high-energy spectrum contains additional structure.

Ten photoelectron spectra were measured over a photon energy range between 480 eV and 1200 eV and were decomposed into the components of the symmetric stretching progression ν_s. The intensity ratios of the $\nu_s = 1$ and $\nu_s = 2$ peaks to the main $\nu_s = 0$ peak are shown in Fig. 2, together with the low-energy data reported in [15]. The dip structure which appears at ~330 eV was attributed to the internal inelastic scattering effect in [15], which becomes
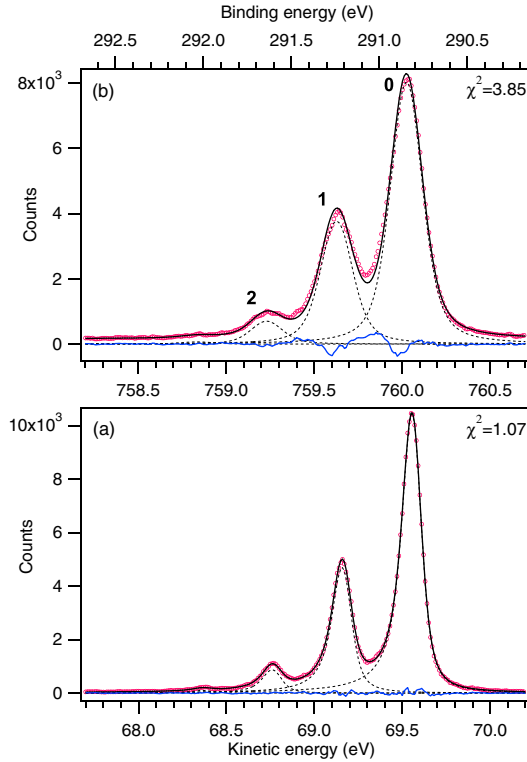
FIG. 1 (color online).   Carbon $1s$ photoelectron spectra of
methane, taken at (a) $h\nu = 360$ eV and (b) $h\nu = 1050$ eV.
Circles—experiment, solid lines—modeled spectra, dashed
lines—individual peaks, labeled by the vibrational quantum
numbers of the symmetric stretch progression. Also the residual
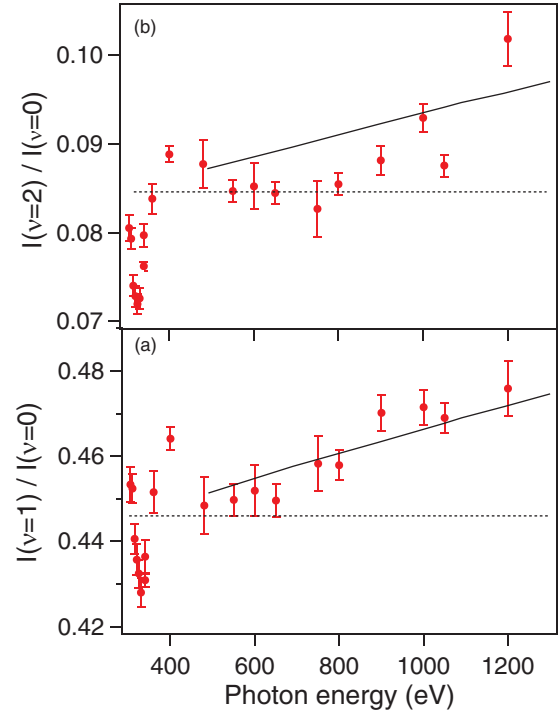of the least-squares fit is shown.

FIG. 2 (color online).   Intensity ratios in the symmetric stretch
progression in C $1s$ photoelectron spectra. Solid line—recoil
model. Dashed line—prediction without recoil.

negligible in the high-energy region above 500 eV. Both
ratios in Fig. 2, however, exhibit an increasing trend even at
higher energies. The literature data with x-ray Al K_α
ionization vary considerably, $I_{\nu_s=1}/I_{\nu_s=0} = 0.54$ [3] and
0.52 [1] versus 0.46 [4]. In addition to the increase of the
intensity ratios with energy, the decomposition of all our
spectra at high photon energy into a single progression
showed visual discrepancies to the measured data, as in
Fig. 1, and an increased value of χ^2. A theoretical expla-
nation for the observed effects in the high-energy spectra is
proposed below.

   According to momentum conservation, the recoil mo-
mentum which the molecule receives from an ejected
photoelectron of kinetic energy E_k is (in atomic units):
$|p_e| = \sqrt{2E_k}$. In the simplest model, the whole molecule
receives this momentum rigidly (elastic recoil). In the case
of core-level photoemission, however, the electromagnetic
field interacts primarily with the atom at which the core
orbital is localized, in a time scale much shorter than the
vibrational period of the molecule. This indicates that the
molecule is unable to receive the recoil momentum rigidly,
but it is rather given to the primary electron emitter—the
carbon atom in our case. Consequently the photoelectron
recoil should be treated on a similar basis to *inelastic*
collision processes that lead to vibrational excitations.

Thus, we will assume that the positions of the nuclei do
not change during the photoemission event and that the
recoil momentum is received by the emitter atom (C) only.

   Whiteley *et al.* [16] studied collisions between diatomic
molecules and massive particles and obtained quantum
mechanical formulas for the vibrational excitation proba-
bilities. They used harmonic oscillator wave functions *in
momentum space*, which is a natural environment for
studying fast, impulsive collisions. One can regard mo-
lecular inner-shell photoemission on the same formal basis.
However, some simplifications can be made, since (i) the
momentum of the incoming particle (photon) is negligible
compared to the momentum of the outgoing particle (elec-
tron), (ii) the mass of the outgoing particle is much smaller
than that of the nuclei, and (iii) photoelectron energy loss
due to recoil is small: $\Delta E_{\text{kin}} \ll E_{\text{kin}}$.

   Let us consider first photoemission from a diatomic
molecule AB, where the photoelectron leaves the atom A
along the molecular (x) axis. The internal coordinate and
momentum of the reduced harmonic oscillator are defined
as $x = x_A - x_B$ and $p = \mu\dot{x}$, where μ is the reduced mass
of the molecule. The departing photoelectron changes the
velocity of the atom A by $\Delta\dot{x}_A = p_e/M_A$, but does not
affect the atom B. Thus $\Delta\dot{x} = \Delta\dot{x}_A$ and, from the momen-
tum conservation, the change in the internal momentum is

$$\Delta p = -\frac{M_B}{M}p_e, \tag{1}$$

where M is the molecular mass. Equation (1) shows that
the lighter the electron emitter A compared to the "specta-

tor'' atom B, the more of the recoil momentum goes into the internal vibrations of the oscillator (inelastic recoil) and the less into translational motion (elastic recoil).

In quantum mechanical interpretation, depositing a momentum Δp into the harmonic oscillator means displacing its initial-state wave function $\psi_0(p)$ along the reduced momentum axis by Δp. The eigenfunctions of the harmonic oscillator in the momentum space are given as [16]:

$$\psi_\nu(p) = N_\nu \exp\left(\frac{-p^2}{2\mu\omega_\nu}\right)H_\nu\left(\frac{p}{\sqrt{\mu\omega_\nu}}\right), \qquad (2)$$

where N_ν are normalization constants, ω_ν vibrational frequencies, and H_ν the Hermite polynomials. The displaced wave function $\psi_0(p + \Delta p)$ is not an eigenfuction of the oscillator anymore, but can be represented as a linear combination of oscillator functions as follows:

$$\psi_0(p + \Delta p) = \sum_\nu c_\nu \psi_\nu(p),$$
$$c_\nu = \langle \psi_\nu(p + \Delta p)\psi_\nu(p)\rangle. \qquad (3)$$

One notices an analogy between Eq. (3) and the Franck-Condon principle formulated in coordinate space. In the latter, vibrational excitations are induced by a shift of the molecular potential along some coordinate, so that the vibrational wave function of the initial state must be presented as an expansion in the new eigenfunctions of the final state. The transition probabilities are given as squares of the expansion coefficients. In the present case, the potential does not change, but the wave function itself is shifted due to recoil momentum. However, the transition probabilities to the final vibrational levels ν are still given by c_ν^2, the squares of the overlap integrals.

In the case of CH_4, the momentum transfer into the internal vibrations is given by Eq. (1) by replacing M_B with $4M_H$. In a classical oscillator, this corresponds to the vibrational excitation energy as: $E_{vib} = (1/M_C - 1/M)E_{kin}$, where M is the molecular mass. For example, with $E_{kin} = 1$ keV, $E_{vib} = 11.4$ meV in CH_4, small but not negligible.

Methane in its core-ionized state has four normal modes, but only the asymmetric stretching (ν_a) and one bending (ν_b) mode involve the motion of the C atom, as sketched in Fig. 3. In order to describe the two modes as one-dimensional harmonic oscillators, we define internal coordinates $R = \frac{1}{4}(R_1 + R_2 - R_3 - R_4)$ and $Q = \frac{1}{4}R_0(\alpha_1 + \alpha_2 - \alpha_3 - \alpha_4)$, ($R_0$—equilibrium bond length and X_C-X coordinate of carbon) and obtain their reduced masses so that

$$\mu_a\dot{R}^2 = 4M_H\dot{R}^2 + M_C\dot{X}_C^2$$
$$\mu_b\dot{Q}^2 = 4M_H\dot{Q}^2 + M_C\dot{X}_C^2, \qquad (4)$$

and the momentum conservation is fulfilled. The total inelastic recoil momentum $\Delta p = (4M_H/M)p_e$ is divided into the internal momenta of the two vibrational modes as $\Delta p_a = \Delta p \cos(\alpha)$ and $\Delta p_b = \Delta p \sin(\alpha)$ (see Fig. 3.)
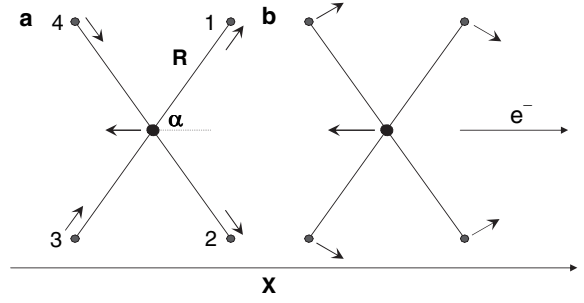

FIG. 3. Schematic of photoemission from a fixed-in-space CH_4 molecule (twisted onto x-y plane for clarity). Shown are the vibrational modes that involve motion of C atom along the x axis, (a) asymmetric stretching, (b) bending.

The following procedure was followed in calculating the probabilities of recoil vibrational excitation. (1) The asymmetric stretching and bending motions of a fixed-in-space molecule were represented by simple harmonic oscillators with reduced masses $\mu_a = 4.50$ amu, $\mu_b = 3.375$ amu, and with the vibrational constants $\omega_a = 0.436$ eV and $\omega_b = 0.183$ eV from Ref. [9]. (2) Vibrational eigenfunctions for these oscillators were constructed in momentum space. (3) The molecule was assumed to be initially in the $\nu = 0$ vibrational state; the corresponding wave function was shifted along the internal momentum axis of the oscillators by Δp_a and Δp_b due to the recoil. (4) Excitation probabilities were calculated as squares of the overlap integrals between the shifted wave function and the eigenfunctions.

A model photoelectron spectrum is shown in Fig. 4 together with an experimental one. The modeled curve was constructed from three progressions (the asymmetric stretching and bending modes as in Fig. 3 and the symmetric stretching), including their combination bands. Excitation probabilities for the first two were calculated by the inelastic recoil model. For the symmetric stretching, in a separate paper [15] we have found the high-energy limit of the probabilities in the absence of recoil as 0.29 and 0.055. The relative peak intensities were taken as products of the probabilities of the three modes. Intensity and energy of the model curve were fitted to the experimental spectrum, using a Gaussian apparatus broadening and a linear background as additional free parameters. The lifetime broadening again was set to 95 meV [8].

The model spectrum has additional intensity between the symmetric stretch progression due to recoil excitations that largely remedies the shortcomings of the fit in Fig. 1(b), as indicated by the significantly reduced χ^2 value and the shape of the residual. Also, the $\nu_s = 1$ and 2 peaks have weak underlying excitations of other vibrational modes. The wave functions of the oscillator representing the bending mode are more compact in the momentum space [Eq. (2)], which leads to higher excitation probabilities than for the asymmetric stretching mode. Furthermore, at the molecular orientation in Fig. 3, the division
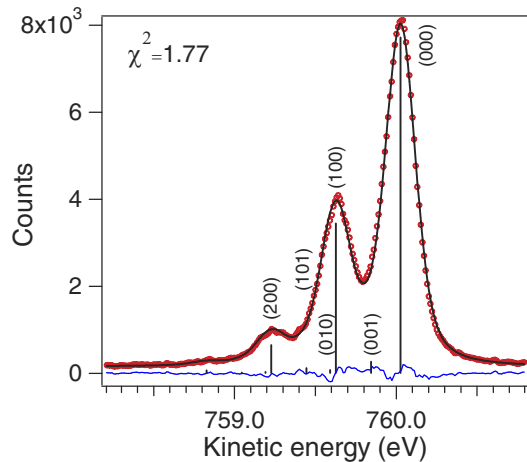
FIG. 4 (color online). Least-squares fit of a modeled C $1s$ photoelectron spectrum to the experiment at $h\nu = 1050$ eV. Vertical bars denote the positions and intensities of the vibrational peaks, with labeling $(\nu_s \nu_a \nu_b)$. Also the residual of the fit is shown.

of the recoil momentum favors the bending mode. Averaging over all molecular orientations can change this division somewhat.

The apparent intensity ratios of the symmetric stretching mode can also be affected by the recoil effects. We modeled the C $1s$ photoelectron spectra at a number of kinetic energies and decomposed them into a single vibrational progression using the same curve-fitting procedure as for the experimental spectra in Fig. 1. The intensity ratios obtained from the modeled spectra are shown in Fig. 2 as a solid line. One can see that by taking into account the recoil excitations the general trend of the experimental observations is explained. We conclude that the apparent increase of the intensity ratios at high kinetic energies is not due to a change in the dominant symmetric stretching progression itself, but reflects an additional underlying structure of other vibrational modes that appears due to the recoil excitations. Although the recoil excitations give minor contribution to the overall vibrational envelope in the present case, in molecules where the electron emitter is surrounded by heavier atoms, the modifications could be much stronger.

Domcke and Cederbaum predicted in their theoretical work a broadening of the vibrational envelope of diatomic molecules due to recoil excitations [17]. This is in agreement with the present approach, as intensity transfer to the higher vibrational levels would also result in an overall broadening of the unresolved envelope.

In Ref. [15] we discuss the non-Franck-Condon behavior in the C $1s$ photoelectron spectrum of CH_4 near the ionization threshold, where the recoil effect is negligible and instead the internal inelastic scattering effect plays a significant role. The latter is molecule-specific while the recoil effect is completely general. We also note that in the intermediate photon energy region ~ 400 eV, where both

the recoil and the inelastic scattering effects are weak, the intensity ratios of the symmetric stretch progression assume a local maximum not explained by either of these formalisms.

In conclusion, the vibrational structure in molecular core-level photoemission is generally described using the Franck-Condon principle, which assumes that neither the positions nor the momenta of the nuclei change during the ionization event. In contrast, in vibrational excitations by collisions with massive particles there is a momentum transfer to the nuclei. We have shown that with the increasing kinetic energy of the emitted electron, core-level photoemission acquires some character of collisional processes due to the recoil effect—in essence, a violation of the Franck-Condon principle takes place. And as the recoil excitation is facilitated by a different mechanism, it involves also the vibrational modes of polyatomic molecules that are inaccessible within the Franck-Condon principle. This could provide means to a more complete experimental information on the potential energy surfaces of core-ionized molecules.

*Electronic address: edwin.kukk@utu.fi
†Electronic address: ueda@tagen.tohoku.ac.jp
 [1] K. Siegbahn, in *Nobel Lectures in Physics 1981–1990,* edited by G. Ekspong (World Scientific, Singapore, 1993).
 [2] L. J. Sæthre *et al.,* J. Am. Chem. Soc. **123,** 10729 (2001).
 [3] U. Gelius *et al.,* Chem. Phys. Lett. **28,** 1 (1974).
 [4] L. Asplund *et al.,* J. Phys. B **18,** 1569 (1985).
 [5] H. M. Köppe *et al.,* Phys. Rev. A **53,** 4120 (1996).
 [6] S. J. Osborne *et al.,* J. Chem. Phys. **106,** 1661 (1997).
 [7] T. D. Thomas *et al.,* J. Chem. Phys. **109,** 1041 (1998).
 [8] T. X. Carroll *et al.,* Phys. Rev. A **59,** 3386 (1999).
 [9] T. Karlsen and K. J. Borve, J. Chem. Phys. **112,** 7986 (2000).
[10] U. Hergenhahn, J. Phys. B **37,** R89 (2004).
[11] K. Ueda, J. Phys. B **36,** R1 (2003).
[12] R. M. Rao *et al.,* Phys. Rev. Lett. **76,** 2666 (1996).
[13] H. Ohashi *et al.,* Nucl. Instrum. Methods Phys. Res., Sect. A **467-468,** 529 (2001).
[14] E. Kukk, Curve fitting macro package SPANCF, http://www.geocities.com/ekukk.
[15] K. Ueda *et al.,* Chem. Phys. Lett. **411,** 33 (2005).
[16] T. W. J. Whiteley *et al.,* J. Phys. B **31,** 2043 (1998).
[17] W. Domcke and L. S. Cederbaum, J. Electron Spectrosc. Relat. Phenom. **13,** 161 (1978).